Geochemistry and Mineralogy of Clays from the Algarve Basin, Portugal: A Multivariate Approach to Palaeoenvironmental Investigations

Maria J. Trindade[1,*], Fernando Rocha[2] and Maria I. Dias[1]

[1]*Instituto Tecnológico e Nuclear / GeoBioTec, EN 10, 2686-953 Sacavém, Portugal;* [2]*GeoBioTec/MIA, Dept. de Geociências. Univ. de Aveiro, Campus de Santiago, 3810-193 Aveiro, Portugal*

Abstract: Lower Cretaceous and Triassic-Hettangian clays from the Algarve Basin (South Portugal) were deposited in distinct environments during basin subsidence due to Pangea break up. The mineralogy, geochemistry and granulometry of 45 samples of both clay groups were studied, using X-ray diffraction, instrumental neutron activation analysis, X-ray fluorescence and laser diffractometry by attenuation of X-rays. Multivariate statistical techniques (principal component analysis and K-means clustering), after scandium normalization of chemical contents, were used to study simultaneously all data, enabling to distinguish the different clay types by establishing the best discriminatory parameters: high contents (in decreased order) of kaolinite, quartz, Chemical Index of Alteration (CIA), Ti, goethite, Hf, Si, > 63 μm fraction and Zr, characterize the group of clays from Cretaceous; while high contents of hematite, Mg, mobile elements (K, Cs and P), illite, Ca, phyllosilicates in general, Mn and dolomite, are associated to Triassic-Hettangian clays. This approach revealed useful to facilitate the integration of all data, as was possible to confront the geochemistry with the mineralogy, enabling the best palaeoenvironmental interpretations. In fact, the clay mineral assemblage is significantly influenced by the dominant weathering process and provides information on changes in aridity/humidity patterns.

Keywords: Algarve Basin, Clays, Geochemistry, Mineralogy, Multivariate analysis, Palaeoenvironments.

1. INTRODUCTION

The Algarve sedimentary basin (South Portugal) (Fig. (**1**)) stands over a Carboniferous low-grade metamorphic basement [1].

Lower Triassic to Upper Cretaceous deposition was controlled by extensional tectonics associated with the breakup of Pangea and development of the Neo-Tethys [2].

Sedimentary environments evolved from continental in the Triassic (red terrigenous siliciclastics) through confined littoral and evaporitic in Triassic-Hettangian to Sinemurian (red shales, dolomites and evaporites), to open marine in Early Pliensbachian (limestones, dolomites and marls) [3]. The rifting phase was manifested by a tholeiitic volcanic event at the Hettangian–Sinemurian transition [4]. During Lower Cretaceous the sedimentation was essentially marine, but was characterized by important facies variations, triggered by more or less pronounced sea-level fluctuations. Intense tectonic movements were responsible for some episodes of siliciclastic fluvial discharges [3].

The main clay-rich units from the basin have been characterized in several works [5-10]. They are illitic clays, exploited through time as common clays to the red ceramic industry up to our days.

The best clay resources are the siliciclastic continental units from Lower Cretaceous, and also the unit of shales, dolomites and evaporites from the Upper Triassic-Hettangian. The larger quarries are localized in Cretaceous units in specific regions of central Algarve, while the Triassic-Hettangian clays have been exploited in smaller and more traditionally factories along a narrow E-W belt that span all over the basin, as shown in Fig. (**1**).

Considering these two types of clays formed under different palaeoenvironmental conditions, the aim of this work is to explore a multivariate solution for geochemical and mineralogical data together, in order to put in evidence those differences and the variables that have greater contribution to their differentiation. The inclusion of the mineral data facilitates the palaeoenvironmental interpretation of the geochemical differences, like the illite/kaolinite ratio related with aridity/humidity changes during the weathering of source rocks.

2. MATERIALS AND METHODS

Twenty-four samples of Cretaceous clays and 21 samples of Triassic-Hettangian clays were used in this study. X-ray fluorescence (XRF) enabled to obtain major elements concentrations as wt% oxides (SiO_2, Al_2O_3, Fe_2O_3t, MnO, MgO, CaO, Na_2O, K_2O, TiO_2, P_2O_5), using fused powder sample with a Li-rich compound and analysed with a Philips PW 1410/00 spectrometer, with CrKα radiation.

Instrumental neutron activation analysis (INAA) was performed at the Portuguese Research Reactor (RPI) allowing to obtain the concentrations of the following trace elements: Sc, Cr, Co, Zn, Ga, As, Br, Rb, Zr, Sb, Cs, Ba, Hf, Ta, W, Th, U, La, Ce, Nd, Sm, Eu, Tb, Yb, Lu. Powdered samples and standard reference materials (GSD-9 and GSS-1 from the Institute of Geophysical and Geochemical Explora-

*Address correspondence to this author at the Instituto Tecnológico e Nuclear. EN 10, 2686-953 Sacavém, Portugal; Tel: +351 21 9946000; Fax: +351 21 9946185; E-mail: mjtrindade@itn.pt; zetrinda@hotmail.com

1573-4110/10 $55.00+.00

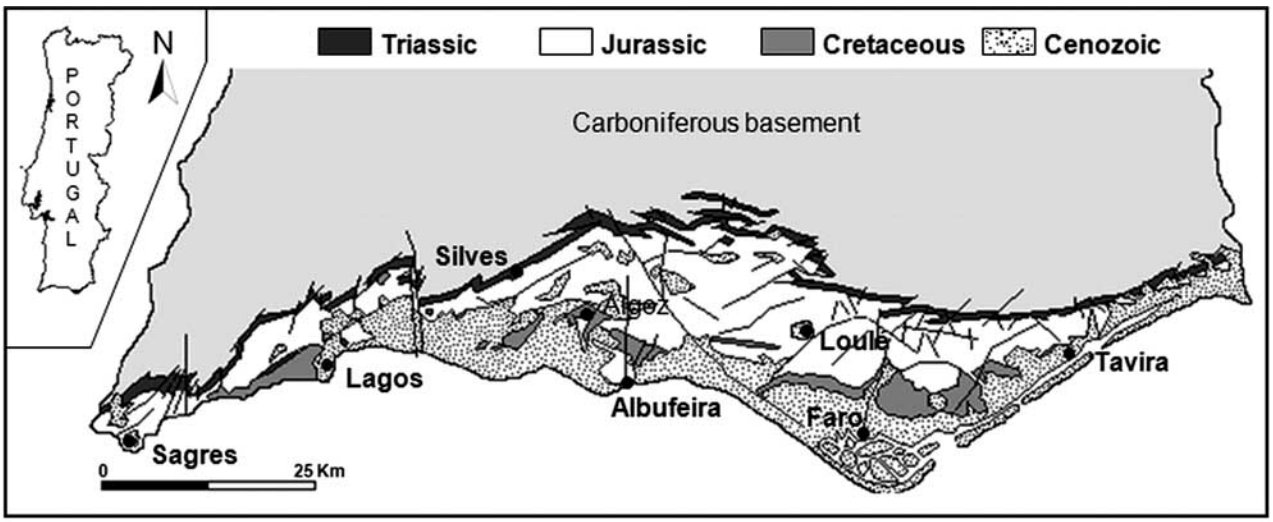

Fig. (1). Simplified geologic map of the Algarve Basin.

tion) were irradiated for six hours, using a thermal flux of 3.589×10^{12} n cm^{-2} s^{-1}, Φ_{th}/Φ_{fast}= 14.14, Φ_{epi}/Φ_{th}= 1.4, and then the γ-spectra was recorded by a high-resolution Ge detector. More details of the INAA method at RPI can be consulted in the literature [11].

The study of non-clay and clay minerals was performed by X-ray diffraction (XRD) on both bulk rock and < 2 μm fraction, respectively. A Phillips X'Pert Pro diffractometer with a PW 3050/6x goniometer and Cu*Kα* radiation, operating at 45 kV and 40 mA, was used.

Clay-sized fraction (< 2 μm) was obtained after decarbonation of calcareous clays, washing with distilled water, centrifugation, sand fraction (> 63 μm) separation by wet sieving and sedimentation according to Stoke's law. Oriented slides were prepared by pipetting the clay+silt suspension on a glass slide. Clay minerals were studied on oriented preparations that were air-dried, ethylene-glycol solvated, heated to 550°C or after subjected to other treatments if necessary.

Semiquantitative estimates of the minerals were achieved by measuring the diagnostic peak areas, considering the full width at half maximum (FWHM), and then weighted by empirically estimated factors [12-15]. The total proportion of clay minerals was estimated taking into account the peak area of the main reflection of phyllosilicates (d = 4.48 Å) in non-oriented preparations, and then the percentages of the various clay minerals were obtained through their diagnostic basal reflections in the glycolated diffractograms.

Granulometry was determined in two steps. Firstly, the sand fraction was obtained by wet sieving and then the particle-size distribution of the silt+clay suspension was measured by laser diffractometry by attenuation of X-rays, using a Micrometrics Sedigraph 5100.

3. RESULTS

The grain size distribution was studied using Shepard's classification [16] that considers the distribution of sediments in three classes: < 2 μm, 2-63 μm and > 63 μm. In general, the materials correspond to silty clays or clayey silts; however, silty clays predominate in Triassic-Hettangian samples, while Cretaceous samples more often correspond to clayey silts or other coarser sediments (sand silt clays and sandy silts).

Estimates of mineral abundances are presented in Table **1**. For comparison of the two clay groups are also shown pie diagrams (Fig. (**2**)) with the average mineralogical composition of the bulk rock and of the clay-sized fraction.

Triassic-Hettangian clays are compositionally more variable than Cretaceous clays, being predominantly formed by phyllosilicates and having quartz, carbonates (mainly dolomite), feldspars, hematite, anatase and anhydrite as accessory minerals. Illite is the main clay mineral and sometimes the only one; smectite and iron-rich chlorites are accessory phases in several samples, and kaolinite is rarely present. Mg-rich minerals (smectite, corrensite, sepiolite, chlorite) were also observed in few samples.

In Cretaceous clays quartz is more abundant than phyllosilicates. Accessory minerals include goethite, alkali feldspar, Ti-oxides (anatase and rutile) and, occasionally, calcite. The clay fraction is mainly formed of illite, but kaolinte is also very abundant (> 30 %). Other clay minerals present in minor quantities are vermiculite, chlorite and smectite. The main differences between samples are quartz/phyllosilicate and illite/kaolinite ratios.

Chemical composition of the Algarve clays is given in Tables **2** and **3**. In addition, some specific chemical parameters are available, namely the Chemical Index of Alteration (CIA) [17], the total rare earth elements content (REE), the europium anomaly (Eu/Eu*), the cerium anomaly (Ce/Ce*) and the chondrite-normalized La/Yb ratio, representing the fractionation between light and heavy rare earths.

The chemistry of the clays is dominated by Si and Al. Cretaceous clays are richer in Si, but have very low Ca and Mg contents, whereas in Triassic-Hettangian clays these elements can be abundant (> 10 %) and they are richer in K. Ca and Mg are associated with carbonates, justifying the higher loss on ignition (LOI) values. Cretaceous clays have

Table 1. Mineral Composition of the Studied Clays Obtained from Semiquantification Based on XRD Data. The Identification of the Minerals was Performed Using ICDD Files

Sample	Bulk Rock Mineralogy													Clay Minerals					
	Qtz	Phy	Cal	Dol	Ank	Afs	Pl	Hem	Gt	Py	Ant	Rt	Anh	Ill	Kln	Sme	Chl	Vrm	Others
CL1	35	57	-	-	-	3	-	-	3	-	2	-	-	67	33	tr	-	-	-
CL2	51	41	-	-	-	2	-	-	1	-	5	-	-	85	15	tr	-	-	Ill-Sme
Et1	54	37	-	-	-	2	3	-	2	-	2	-	-	69	31	-	-	tr	Ill-Vrm
Et2	41	33	-	-	-	2	3	-	4	-	16	1	-	70	27	3	-	-	Ill-Sme
SL1	35	55	-	-	-	2	1	-	2	-	5	-	-	72	27	1	tr	-	-
SL2	59	36	-	-	-	-	1	-	2	-	2	-	-	58	38	1	-	3	-
SL3	58	34	-	-	-	1	3	-	2	-	1	1	-	66	29	-	-	5	-
MM1	39	55	-	-	-	1	1	-	2	-	1	1	-	65	35	-	-	-	-
MM2	63	25	-	-	-	2	2	-	3	-	4	1	-	71	29	-	tr	-	-
MM3	54	41	-	-	-	1	1	-	1	-	2	-	-	59	41	-	-	-	-
MM4	66	32	-	-	-	1	-	-	-	-	1	-	-	38	62	-	-	-	-
MM5	66	30	-	-	-	1	1	-	-	-	1	1	-	60	40	-	-	-	-
Pc1	71	22	2	-	-	2	1	-	-	-	2	-	-	88	8	-	4	-	-
Pc2	69	15	12	-	-	1	1	-	1	-	1	-	-	75	20	-	5	-	-
Va1	34	60	-	-	-	1	1	-	2	-	1	1	-	71	28	-	-	1.0	-
Va2	56	30	-	-	-	2	3	-	5	-	2	2	-	58	42	-	-	-	-
Va3	40	47	-	-	-	2	2	-	5	-	3	2	-	73	27	-	-	-	-
Va4	43	50	-	-	-	2	1	-	-	1	2	1	-	64	36	-	-	-	-
Va7	64	22	-	-	-	2	2	-	3	-	2	5	-	71	29	-	-	-	-
Va8	52	41	-	-	-	1	2	-	2	-	1	1	-	62	38	-	-	-	-
VS1	68	20	-	-	-	1	2	-	5	-	2	2	-	56	38	-	-	6.0	-
VS2	64	30	-	-	-	-	2	-	1	-	2	1	-	67	33	-	-	-	-
VS3	58	32	-	-	-	2	2	-	3	-	3	-	-	75	25	-	-	-	-
VS4	51	44	-	-	-	1	1	-	-	1	2	-	-	61	39	-	-	-	-
Al3	28	52	2	11	-	-	3	2	-	-	-	-	2	97	3	-	-	-	-
BSJ1	34	37	8	10	-	3	4	2	-	-	2	-	-	87	-	7	6	-	-
BSJ2	7	86	4	-	-	-	1	1	-	-	1	-	-	99	-	1	-	-	-
BSJ3	9	77	3	2	-	3	3	-	-	-	3	-	-	90	-	-	10	-	-
CM2	15	75	-	2	-	1	3	2	-	-	2	-	-	100	-	-	-	-	-
CM3	10	59	-	24	-	1	2	2	-	-	1	-	1	100	-	-	-	-	-
CM4	27	48	-	11	-	2	5	4	-	-	3	-	-	99	1	-	-	-	-
Crd1	18	72	7	-	-	1	-	1	-	-	1	-	-	93	-	1	6	-	-
Es1	11	62	-	19	-	1	2	2	-	-	3	-	-	100	-	-	-	-	-
Es2	17	75	1	1	-	1	2	2	-	-	1	-	-	99	1	-	-	-	-
Es3	16	76	-	1	-	1	2	2	-	-	2	-	-	100	-	-	-	-	-

(Table 1) contd....

Sample	Bulk Rock Mineralogy													Clay Minerals					
	Qtz	Phy	Cal	Dol	Ank	Afs	Pl	Hem	Gt	Py	Ant	Rt	Anh	Ill	Kln	Sme	Chl	Vrm	Others
Pte1	12	70	5	2	-	6	-	1	-	-	4	-	-	70	-	23	7	-	-
RA1	20	37	-	38	-	1	1	1	-	-	-	-	2	98	tr	-	2	-	-
SCB5	31	39	23	-	-	1	-	2	-	-	3	-	1	69		16	15	-	-
SCB6	22	67	-	3	-	2	3	1	-	-	2	-	-	100	tr	-	-	-	-
Sv1	4	69	-	18	-	-	-	3	-	-	6	-	-	100	tr	-	-	-	-
Tor1	4	20	1	70	-	2	-	2	-	-	-	-	1	96	4	-	-	-	Sep
VA1	10	75	2	7	-	2	2	1	-	-	-	-	1	98	-	-	2	-	Cor
Vboi1	17	56	3	7	10	4	-	1	-	-	2	-	-	70	-	19	11	-	-
VBoi2	14	60	11	-	2	6	-	1	-	-	5	-	1	80	-	9	11	-	-
VlB1	1	67	2	26	-	2	-	1	-	-	-	-	1	45	-	55	-	-	Chl-Vrm

Mineral abbreviations: Qtz (quartz); Phy (phyllosilicates); Cal (calcite); Dol (dolomite); Ank (ankerite); Afs (alkali-feldspar); Pl (plagioclase); Hem (hematite); Gt (goethite); Py (pyrite); Ant (anatase); Rt (rutile); Anh (anhydrite); Ill (illite); Kln (kaolinite); Sme (smectite); Chl (chlorite); Vrm (vermiculite); Sep (sepiolite); Cor (corrensite); Ill-Sme (mixed layered illite-smectite); Ill-Vrm (mixed layered illite-vermiculite); Chl-Vrm (mixed layered chlorite-vermiculite).

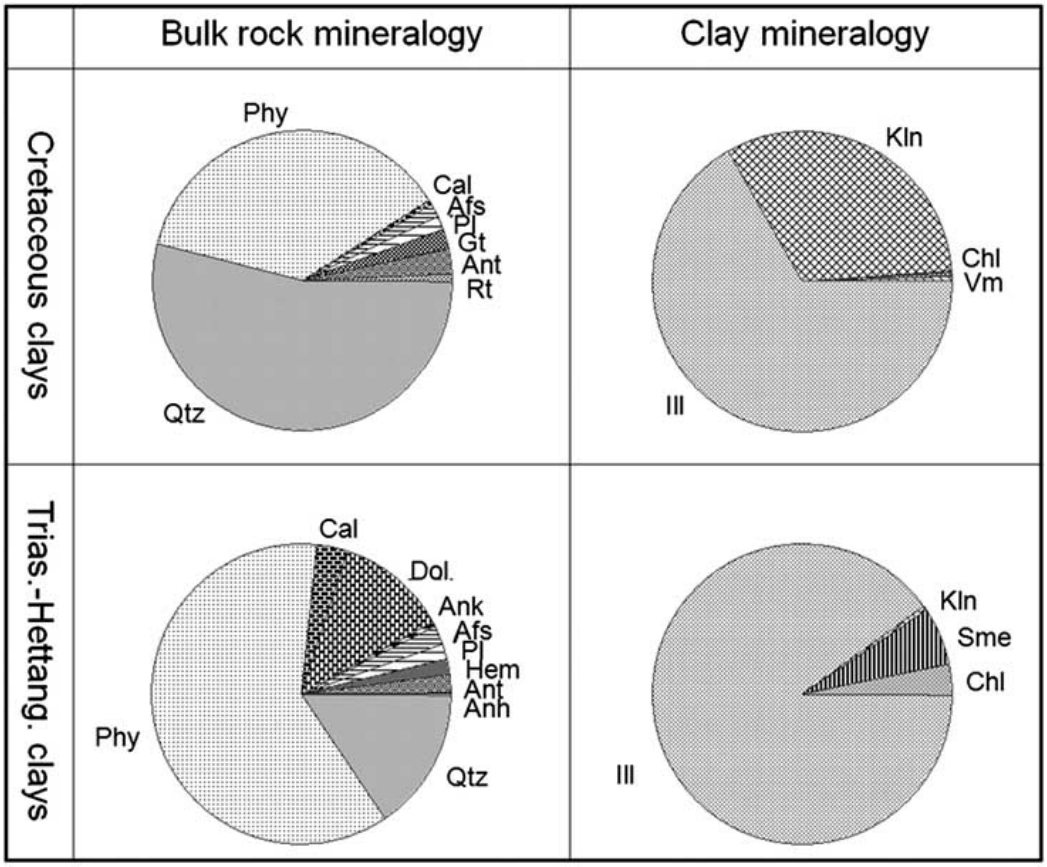

Fig. (2). Pie diagrams with average mineralogical composition. Mineral abbreviations are the same of Table **1**.

higher CIA values than Triassic-Hettangian clays (82 % and 57 %, respectively).

Incompatible/compatible element ratios (La/Sc, Th/Cr, Th/Sc and Zr/Sc) show that clayey materials resulted from weathering of continental crust; however we observed felsic/mafic compositional variations in the source area of the more olden clays. In addition, clays resulted from intense recycling and mixture of sediments and sedimentary calibration, with enrichment of coarser fractions in heavy minerals such as zircon.

Table 2. Major (in wt.%) and Trace (in mg/g) Element Contents and Other Chemical Parameters of the Studied Clays from Cretaceous. The Meaning of the Symbols used is: LOI - Loss on Ignition; CIA - Chemical Index of Alteration; REE - Total Rare Earth Elements Content; Eu/Eu* - Europium Anomaly; Ce/Ce* - Cerium Anomaly and (La/Yb)n - Chondrite-Normalized Lanthanum and Ytterbium Ratio

	CL1	CL2	Et1	Et2	SL1	SL2	SL3	MM1	MM2	MM3	MM4	MM5	Pc1	Pc2	Va1	Va2	Va3	Va4	Va7	Va8	VS1	VS2	VS3	VS4
SiO_2	60.4	63.5	64.7	56.6	63.0	75.5	69.2	68.6	68.3	71.5	81.9	81.3	74.0	72.5	66.5	62.0	62.4	64.6	66.3	68.1	64.4	75.3	68.3	70.5
Al_2O_3	15.3	14.9	18.5	20.6	18.6	12.7	16.8	14.4	14.4	16.4	10.3	10.5	11.9	9.50	16.5	18.3	22.1	20.7	16.4	14.8	14.1	10.7	15.2	17.4
Fe_2O_3(t)	10.8	8.48	5.33	6.86	6.65	4.12	3.88	6.44	6.88	1.68	0.54	0.51	2.72	3.38	5.03	6.95	2.10	1.77	5.62	5.90	9.99	5.69	5.79	1.46
MnO	0.22	0.03	n.d.	n.d.	n.d.	n.d.	n.d.	0.02	0.01	0.01	0.01	n.d.	0.02	0.03	0.03	0.06	0.02	0.01	0.02	0.03	0.08	0.05	0.04	0.01
MgO	1.25	1.44	0.66	0.53	0.65	0.29	0.76	0.50	0.45	0.44	0.28	0.29	0.92	0.61	0.72	0.76	0.61	0.52	0.50	0.65	0.70	0.42	0.77	0.48
CaO	0.54	0.39	0.01	n.d.	n.d.	n.d.	0.01	0.07	0.05	0.06	0.08	0.04	1.38	4.15	0.17	0.17	0.14	0.08	0.11	0.11	0.14	0.14	0.15	0.03
Na_2O	0.44	0.39	0.11	3.84	0.03	n.d.	n.d	0.35	0.29	0.77	0.32	0.17	0.33	0.22	0.57	0.33	0.92	0.90	0.76	0.73	0.29	0.25	0.40	0.44
K_2O	3.97	4.51	3.98	4.08	4.31	2.47	3.73	2.08	2.26	2.36	0.99	1.30	2.70	1.90	2.55	2.46	2.66	2.54	1.92	1.97	1.75	1.29	2.31	2.22
TiO_2	0.98	1.14	1.44	1.33	1.36	0.98	1.54	1.29	1.05	1.15	0.74	1.42	1.24	0.98	1.18	1.15	1.23	1.25	1.27	1.26	1.20	1.01	1.19	1.26
P_2O_5	0.02	0.02	0.02	0.12	n.d.	n.d.	n.d.	0.05	0.04	0.05	0.04	0.05	0.01	0.02	0.04	0.03	0.04	0.04	0.04	0.04	0.04	0.03	0.04	0.06
LOI	6.10	5.20	5.30	6.10	5.40	4.00	4.20	5.00	5.00	4.50	3.70	3.20	4.80	6.70	5.90	6.30	6.90	6.70	6.00	5.20	6.10	3.90	5.40	5.0
Total	100.0	100.0	100.0	100.0	100.1	100.1	100.1	98.8	98.8	99.0	98.9	98.7	100.0	100.0	99.2	98.54	99.1	99.1	99.0	98.8	98.7	98.8	99.6	98.9
Sc	15.0	15.2	21.0	25.7	21.6	12.5	18.0	13.9	15.5	15.8	10.4	11.9	13.4	10.7	17.0	18.8	23.4	19.1	14.0	16.4	15.6	10.1	14.4	16.5
Cr	73.7	82.2	97.4	124	97.9	64.6	83.9	69.7	76.9	83.5	67.4	59.3	63.4	50.6	88.7	92.6	125	105	73.2	94.3	79.5	59.9	79.2	90.6
Co	14.3	15.8	5.85	6.81	4.30	4.69	16.2	12.8	5.90	2.85	8.33	1.48	20.0	8.96	12.3	14.8	13.5	27.0	7.41	9.97	34.2	15.6	20.3	2.66
Zn	153	69.1	24.7	33.5	23.7	29.5	86.1	49.5	42.1	35.0	33.2	n.d.	80.2	62.8	40.5	53.5	48.7	117	37.8	36.4	59.6	27.5	41.6	31.3
Ga	12.1	14.3	14.5	16.9	15.2	8.55	12.1	12.6	16.0	13.6	7.49	8.35	13.9	11.6	20.9	24.1	9.70	19.3	14.6	11.1	19.1	8.06	12.0	12.7
As	21.7	31.0	3.34	20.3	2.17	4.85	4.82	7.84	9.71	1.53	2.15	3.73	5.15	4.09	8.54	9.84	8.76	23.4	6.82	7.92	11.2	7.07	5.53	12.1
Br	0.675	1.35	2.06	4.52	4.21	1.56	1.70	3.28	1.05	0.526	0.605	1.63	2.92	2.92	8.34	5.72	1.27	n.d.	4.81	5.19	3.40	2.18	11.9	0.983
Rb	119	133	125	133	137	82.1	120	83.0	99.9	102	46.4	59.0	93.7	73.3	112	124	144	131	90.9	95.1	83.6	60.6	100	92.6
Zr	211	198	212	206	203	158	224	229	192	236	208	320	243	227	206	179	143	155	241	179	241	314	245	350
Sb	1.13	1.66	0.582	1.58	0.493	0.734	0.775	0.913	1.10	0.683	0.731	0.862	0.736	0.835	0.938	1.13	1.37	1.73	1.10	1.05	1.50	1.21	1.18	1.14
Cs	7.29	8.00	8.97	9.51	9.14	5.18	6.48	6.42	7.27	7.82	4.31	4.14	6.03	4.94	7.94	8.60	11.7	10.1	7.19	8.09	5.70	4.11	6.53	7.5.0
Ba	441	348	359	603	420	276	373	168	178	229	215	161	205	211	176	238	328	242	336	320	211	220	179	219
Hf	5.79	6.04	6.41	5.21	5.47	4.79	7.19	7.25	7.12	7.84	5.39	9.82	7.12	6.93	6.66	5.45	5.49	6.51	6.9	6.75	7.5	9.45	7.64	10.8
Ta	1.06	1.20	1.40	1.30	1.19	0.828	1.47	1.37	1.22	1.31	0.869	1.57	1.46	1.16	1.40	1.38	1.50	1.53	1.31	1.46	1.41	1.05	1.19	1.48
W	1.20	1.78	1.98	1.67	1.68	1.25	1.97	1.99	1.96	1.71	0.999	1.84	1.91	1.47	2.36	2.02	1.83	2.35	1.64	1.80	2.05	1.53	2.08	2.26
Th	9.57	10.8	12.5	14.6	13.0	8.78	13.2	11.0	10.3	11.3	7.39	12.8	10.7	9.04	11.5	12.6	14.0	14.0	10.9	12.3	11.8	8.38	10.5	12.3
U	3.13	3.31	3.66	3.90	3.33	1.96	3.11	2.55	2.12	2.47	2.52	2.55	2.26	1.56	2.09	2.90	8.34	8.93	2.37	2.53	2.43	1.83	2.03	3.24
La	27.3	33.5	32.8	103	30.0	20.4	46.8	27.7	26.4	28.1	36.6	36.2	30.0	29.0	27.0	41.3	51.3	51.7	30.7	40.4	34.9	30.3	40.6	45.7
Ce	78.1	60.7	57.2	119	49.8	34.6	85.3	41.8	49.0	52.0	76.7	85.5	58.1	58.4	49.4	79.4	97.2	94.3	60.2	75.0	97.1	61.5	48.5	108
Nd	31.4	28.9	25.0	78.7	25.7	17.5	47.0	18.0	21.9	23.8	36.4	44.0	25.6	25.2	23.4	38.5	49.2	45.4	28.9	35.6	37.6	28.8	41.3	47.6
Sm	6.40	6.37	4.61	13.7	4.16	2.98	7.64	4.78	4.15	4.39	6.96	8.32	4.37	4.55	4.81	7.37	8.57	8.53	5.21	6.50	11.7	8.14	10.1	12.6
Eu	1.63	1.43	0.953	3.19	0.886	0.691	1.66	0.995	0.864	0.928	1.46	1.61	1.07	1.07	1.05	1.53	1.87	1.69	1.04	1.36	1.68	1.15	1.48	1.76

(Table 2) contd...

	CL1	CL2	Et1	Et2	SL1	SL2	SL3	MM1	MM2	MM3	MM4	MM5	Pc1	Pc2	Va1	Va2	Va3	Va4	Va7	Va8	VS1	VS2	VS3	VS4
Tb	0.984	0.945	0.774	1.5.0	0.695	0.467	1.11	0.728	0.698	0.772	0.922	1.08	0.769	0.805	0.878	0.974	1.03	1.07	0.659	0.857	1.16	0.767	1.01	1.06
Yb	3.04	3.22	3.04	3.60	2.75	1.61	2.58	3.05	2.94	3.11	2.59	3.79	3.01	2.63	3.41	3.37	3.27	3.49	2.75	3.11	4.05	3.04	3.48	4.00
Lu	0.470	0.503	0.490	0.541	0.520	0.359	0.712	0.434	0.414	0.422	0.411	0.501	0.453	0.42	0.457	0.462	0.499	0.474	0.381	0.469	0.542	0.412	0.46	0.578
CIA	75.5	73.8	81.9	72.2	81.1	83.7	81.8	85.2	84.7	83.7	88.0	87.4	73.0	60.2	83.4	86.1	85.6	85.5	85.5	84.0	86.6	86.5	84.2	86.6
REE	18.7	16.9	15.6	40.4	14.3	9.82	24.1	12.2	13.3	14.2	20.3	22.6	15.4	15.3	13.8	21.6	26.6	25.8	16.2	20.4	23.6	16.8	18.4	27.7
Eu/Eu*	0.796	0.710	0.627	0.815	0.647	0.720	0.692	0.652	0.631	0.631	0.689	0.640	0.731	0.701	0.644	0.682	0.740	0.662	0.666	0.688	0.519	0.520	0.528	0.533
Ce/Ce*	1.25	0.871	0.874	0.578	0.800	0.817	0.833	0.797	0.904	0.896	0.961	1.01	0.934	0.966	0.878	0.901	0.880	0.871	0.915	0.886	1.24	0.945	0.544	1.07
(La/Yb)n	5.44	6.31	6.54	17.3	6.61	7.68	11.0	5.50	5.44	5.48	8.56	5.79	6.04	6.68	4.80	7.43	9.51	8.98	6.77	7.87	5.22	6.04	7.07	6.92

CIA = [Al2O3/(Al2O3+CaO+Na2O+K2O)] x 100

Table 3. Major (in wt.%) and Trace (in mg/g) Element Contents and Other Chemical Parameters of the Triassic-Hettangian Clays. Symbols are According to Table 2

	Al3	BSJ1	BSJ2	BSJ3	CM2	CM3	CM4	Crd1	Es1	Es2	Es3	PTe1	RA1	SCB5	SCB6	Sv1	Tor1	VA1	VBoi1	VBoi2	VlB1
SiO_2	53.7	48.5	51.9	52.6	54.7	45.5	52.7	55.6	42.1	55.7	55.9	51.1	41.8	44.6	52.1	44.4	22.3	44.4	48.2	47.6	36.9
Al_2O_3	16.8	13.1	16.5	15.8	19.1	16.4	17.7	15.1	15.3	18.1	15.5	13.3	11.1	12.3	18.5	17.7	6.70	12.4	12.2	14.5	11.8
Fe_2O_3(t)	6.98	6.54	8.45	5.69	7.90	7.10	7.25	5.88	7.08	7.51	4.08	8.14	5.19	9.56	12.0	9.57	8.44	10.5	5.03	6.71	9.80
MnO	0.06	0.14	0.06	0.09	0.05	0.15	0.08	0.31	0.18	0.06	0.14	0.09	0.21	0.02	0.06	0.14	0.07	0.21	0.13	0.08	0.07
MgO	3.12	8.82	6.27	6.92	2.20	5.16	3.03	5.80	5.81	2.06	3.63	8.87	7.84	4.72	2.12	5.87	12.3	8.20	8.46	5.94	9.33
CaO	3.45	5.12	1.92	2.70	0.78	5.62	2.29	3.24	7.31	1.90	3.93	3.48	10.9	10.6	1.55	3.50	19.6	6.56	7.38	7.89	9.05
Na_2O	0.33	0.47	0.51	0.58	0.36	0.31	0.34	0.31	1.32	1.95	1.70	0.63	0.29	1.42	n.d.	0.34	n.d.	n.d.	0.27	0.29	0.38
K_2O	5.32	4.03	5.40	5.7	6.83	6.27	6.71	4.68	5.22	5.62	5.06	5.01	2.81	3.17	6.29	6.81	2.99	5.63	3.78	4.48	3.54
TiO_2	0.92	0.76	0.93	0.91	0.97	0.75	1.01	0.75	0.81	0.96	0.89	0.97	0.76	1.09	1.24	0.68	0.62	1.00	0.73	0.76	0.74
P_2O_5	0.23	0.19	0.17	0.21	0.16	0.20	0.17	0.14	0.21	0.15	0.22	0.11	0.11	0.09	0.10	0.13	0.03	0.12	0.12	0.12	0.02
LOI	9.10	11.0	7.60	8.50	6.30	12.4	8.30	8.20	14.7	6.70	9.30	8.30	18.4	12.0	6.10	10.9	27.0	11.0	13.7	11.6	18.4
Total	99.9	98.7	99.7	99.7	99.4	99.9	99.5	100.0	100.0	100.7	100.3	100.0	99.4	99.6	100.1	100.0	100.1	100.1	100.0	100.0	100.0
Sc	15.6	14.3	17.4	16.7	18.3	15.6	16.7	15.3	15.4	16.9	15.9	13.4	11.6	16.5	18.2	15.5	18.2	15.1	12.7	14.1	31.0
Cr	88.6	81.7	87.7	103	81.9	69.1	77.2	67.7	79.6	89.4	82.9	68.7	55.3	82.6	79.5	80.1	53.9	86.0	67.8	70.7	144
Co	19.5	17.9	16.1	15.6	12.2	14.1	12.7	21.0	10.9	11.0	16.2	15.7	16.8	15.8	11.5	18.3	8.32	25.4	14.7	17.3	17.7
Zn	52.2	94.1	87.3	83.4	53.8	48.4	51.5	92.7	38.6	45.9	44.3	85.1	52.0	49.7	39.2	101	20.8	93.0	94.0	93.6	113
Ga	13.0	10.1	13.4	18.0	17.9	19.7	22.8	19.0	12.4	12.7	9.51	20.9	14.2	10.4	17.2	27	6.19	10.5	13.0	15.9	11.9
As	19.5	10.2	8.85	8.93	24.0	12.9	8.73	8.55	6.98	6.53	4.09	9.06	38.1	5.48	13.1	3.02	1.44	4.50	3.85	12.3	1.69
Br	2.14	0.763	1.93	1.16	1.99	3.68	1.84	1.57	4.84	2.02	3.38	5.93	5.32	3.99	1.42	1.93	10.2	4.78	2.55	1.83	9.35
Rb	132	97.4	130	133	169	152	162	122	143	155	135	108	106	85.6	169	191	54.6	103	89.3	110	68.3
Zr	247	162	171	130	195	153	154	117	104	172	191	158	157	170	180	53.7	67.4	152	213	163	62.2
Sb	1.11	0.648	0.430	0.347	1.18	1.05	0.98	0.773	0.907	1.08	0.634	0.629	0.747	0.34	1.15	0.842	n.d.	0.615	0.602	0.61	n.d.
Cs	26.3	18.3	29.3	30.2	40.9	36.0	46.4	19.1	51.1	44.1	39.7	19.3	55.1	6.19	45.5	45	3.15	18.7	20.6	20.3	14.9

(Table 3) contd...

	Al3	BSJ1	BSJ2	BSJ3	CM2	CM3	CM4	Crd1	Es1	Es2	Es3	PTe1	RA1	SCB5	SCB6	Sv1	Tor1	VA1	VBoi1	VBoi2	VlB1
Ba	559	276	341	233	794	386	467	455	329	827	1505	397	413	416	402	274	65.6	477	285	263	65.0
Hf	5.80	4.39	4.10	4.73	4.65	3.87	4.61	4.36	3.83	4.79	5.34	4.77	4.46	4.84	4.28	2.67	1.24	3.77	5.20	4.40	1.84
Ta	1.41	1.05	1.22	1.29	1.43	1.07	1.45	1.19	1.21	1.48	1.31	1.11	1.01	1.12	1.49	1.12	0.239	0.994	1.01	1.18	0.399
W	2.67	0.938	1.45	1.36	1.63	1.71	1.71	1.74	1.64	1.94	1.74	1.09	1.23	1.15	2.38	1.62	0.303	0.931	1.08	1.39	0.337
Th	13.7	8.68	9.96	10.3	14.0	11.4	14.4	11.2	11.9	13.8	13.5	9.52	9.47	9.47	14.2	9.83	1.68	8.43	8.71	10.9	2.28
U	5.58	1.59	2.26	2.94	2.37	2.13	2.68	2.17	3.19	2.77	2.96	2.17	1.72	1.80	3.46	2.67	0.791	2.30	1.87	1.84	1.03
La	49.8	32.0	31.1	31.7	50.3	35.6	49.4	30.3	39.9	46.7	44.7	35.3	35.8	34.2	47.4	30.5	6.55	35.3	31.2	39.5	6.62
Ce	96.4	63.2	61.2	62.4	95.1	69.6	94.0	69.0	77.8	91.1	86.4	68.2	66.9	68.9	92.6	59.5	13.9	108	59.7	73.5	11.7
Nd	42.1	31.3	31.0	30.4	58.0	31.9	43.0	32.0	40.1	44.6	43.9	31.5	34.9	34.0	40.5	26.0	9.42	35.5	26.4	32.5	7.34
Sm	7.87	5.68	6.05	6.14	7.66	6.69	8.40	6.28	6.98	7.79	8.02	6.21	6.49	5.96	8.13	4.74	2.23	5.33	5.39	6.25	1.89
Eu	1.7	1.29	1.33	1.41	1.58	1.39	1.74	1.38	1.56	1.69	1.78	1.32	1.36	1.33	1.66	1.05	0.709	1.19	1.17	1.32	0.619
Tb	1.01	0.767	0.822	0.837	1.01	0.935	1.01	0.828	0.939	1.03	1.11	0.872	0.911	0.882	0.95	0.57	0.413	0.677	0.727	0.817	0.436
Yb	3.25	2.42	2.48	2.55	3.01	2.77	3.41	2.59	2.85	3	2.31	2.47	2.88	2.76	3.05	1.82	1.43	2.08	2.38	2.48	1.59
Lu	0.493	0.369	0.398	0.39	0.531	0.449	0.589	0.403	0.402	0.451	0.476	0.342	0.427	0.414	0.47	0.305	0.23	0.316	0.382	0.406	0.403
CIA	64.8	57.7	67.8	63.8	70.6	57.4	65.4	64.8	52.4	65.6	59.2	59.3	44.3	44.7	70.3	62.4	22.9	50.4	51.6	53.4	47.7
REE	25.3	17.1	16.8	17.0	27.1	18.7	25.2	17.9	21.3	24.5	23.6	18.3	18.7	18.6	24.3	15.6	4.4	23.5	15.9	19.6	3.8
Eu/Eu*	0.717	0.741	0.716	0.747	0.678	0.670	0.702	0.723	0.730	0.713	0.718	0.684	0.675	0.706	0.699	0.751	0.933	0.743	0.708	0.696	0.894
Ce/Ce*	0.937	0.911	0.901	0.914	0.825	0.928	0.912	1.02	0.891	0.907	0.890	0.918	0.863	0.924	0.941	0.941	0.860	1.40	0.926	0.909	0.783
(La/Yb)n	9.29	8.01	7.60	7.53	10.1	7.79	8.78	7.09	8.48	9.43	11.7	8.66	7.53	7.51	9.42	10.2	2.78	10.3	7.94	9.65	2.52

Chondrite-normalized rare earths' patterns are typical of upper continental crust, characterized by fractionation between light and heavy rare earths and by a negative europium anomaly.

4. DISCUSSION

4.1. Multivariate Analysis

Multivariate statistical analysis was employed using the Statistica program [18], in order to characterize and differentiate possible clay groups. Principal component analysis (PCA) and K-means clustering were performed after Sc (conservative element) normalization of chemical contents. This procedure allow to compensate for the influence of natural processes, such as grain-size distribution and mineralogy effects on trace element concentrations, thus diminishing erroneous interpretation of clays characterization and differentiation [19]. In the chemometric analysis the whole data set (mineralogical, geochemical and granulometric data) was used, resulting in one matrix of 54 variables × 45 cases. The preprocessing used was autoscale, which involves mean centering and variance scaling of the data.

The loadings and scores provided by PCA are shown in Fig. (**3**). The first two components supply more than 40 % (PC1 = 26.3 %; PC2 = 15.6 %) of the information, being the first principal component (PC1) the main responsible for the separation between the Triassic-Hettangian clays and the Cretaceous clays, the first one projecting along the positive side (PC1+) and the second one along the negative side (PC1-). The most contributing components to the definition of this component are, in decreased order of importance: Mg, Ca, hematite, K, Eu/Eu*, illite, dolomite, phyllosilicates, Cs and P (PC1+); and quartz, CIA, kaolinite, Ti, Hf, Si, Zr, Sb, W and > 63 μm (PC1-). Also PC2 enable to distinguish the two types of clays; Triassic-Hettangian clays are majority located in the positive side of PC2, defined mainly by Rb, Th, Al, REE, Ta, P, Cs and K, whereas Cretaceous clays tend to be sited in the negative side of PC2. The two clays Tor1 and VlB1 from Triassic-Hettangian age have a very different composition of the remaining and can be considered as outliers. In fact, they present much higher dolomite, smectite and Sc contents (not seen due to Sc-normalization of chemical contents; see Table **2**) and the absence of europium anomaly (Eu/Eu* values near the unit). These two samples resulted from chemical weathering of more mafic sources [9].

Other components account for small variations in the composition of both clay groups, although they have no role in their differentiation.

Considering that the Triassic-Hettangian clays and the Cretaceous clays define two independent groups, even including the two outlier samples, as seen from PCA, we can

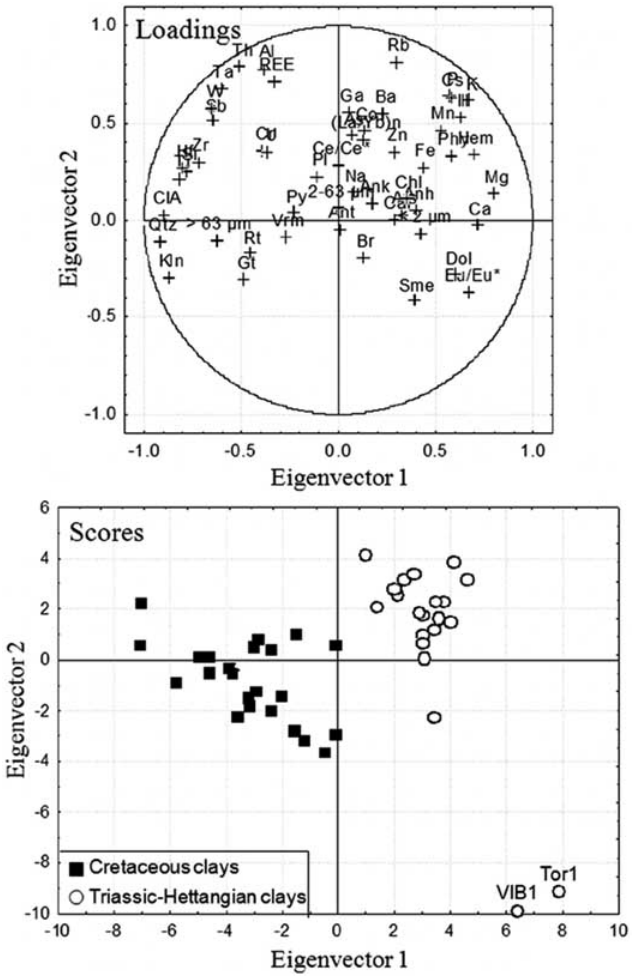

Fig. (3). PCA of variables and samples for the Cretaceous and Triassic clays. Mineral abbreviations are the same used in Table **1**.

use K-means clustering, another unsupervised method, to produce exactly two different clusters of greatest possible distinction, and examine the means for each cluster on each dimension to assess how distinct our groups are and which variables contribute more for that distinction, validating the conclusions obtained before.

Fig. (**4**) shows K-means clustering with variables arranged in order to facilitate the interpretation of the graph. The clusters obtained correspond exactly to the two types of clays: Cluster 1 = Triassic-Hettangian clays and Cluster 2 = Cretaceous clays.

The magnitude of the *F* values from the analysis of variance (between and within clusters) performed on each variable is indicative of how well the respective variable discriminates between clusters. Taking into account the *F* values we can order the variables by decrease of importance in defining the two clusters, according to Table **4**.

The elements, minerals and granulometric classes presented in the previous table are the best discriminator parameters or fingerprints that enable the best differentiation between Triassic-Hettangian and Cretaceous clays. The underlined components (hematite, Mg, P, K, Cs, illite, Ca, phyllosilicates, Mn and dolomite) are higher in the Triassic-Hettangian clays, whereas high contents of the not underlined ones (kaolinite, quartz, CIA, Ti, goethite, Hf, Si, > 63 μm, Zr, Sb, Rt) characterize the Cretaceous clays.

4.2. Palaeoenvironmental Interpretation

Some palaeoenvironmental considerations arise from the tracers obtained by multivariate analysis, which enabled a complete distinction of the clays.

Triassic-Hettangian clays have high contents of Mg and Ca that are mainly present in dolomite, related with the evaporitic conditions prevailing during deposition in the incipient basin. From Triassic to Lower Jurassic, the early

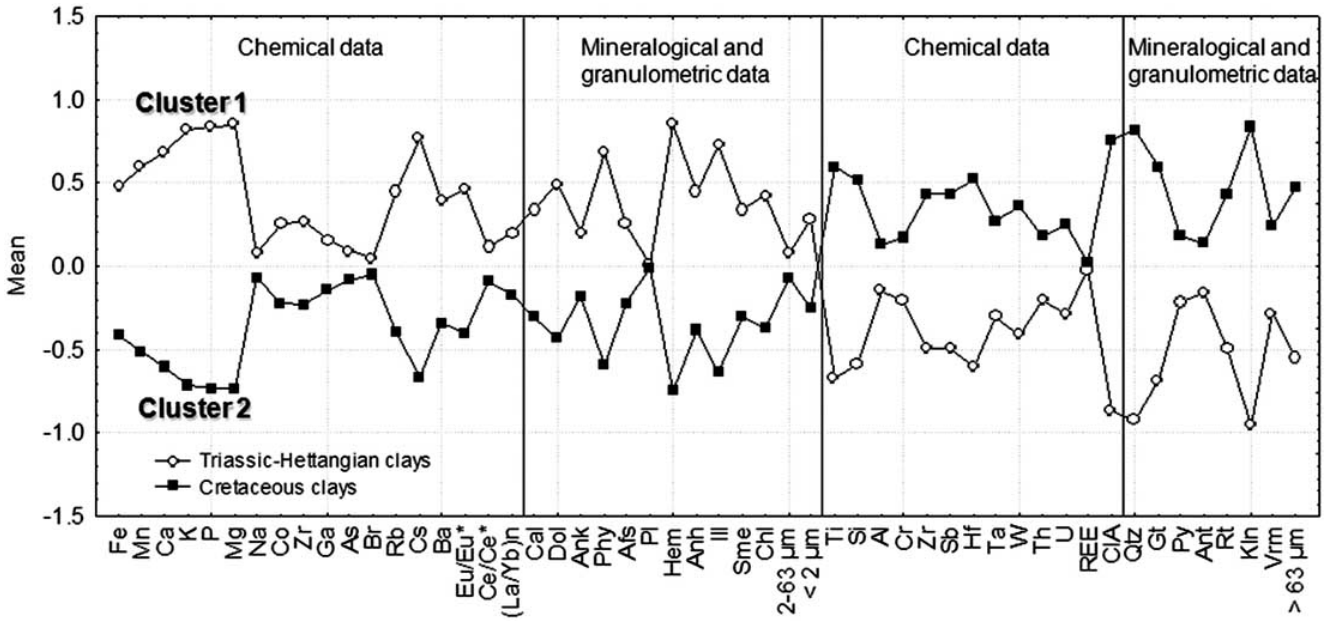

Fig. (4). Plot of means for each cluster on K-means clustering. Mineral abbreviations are according to Table **1**.

Table 4 . Values of the Parameter *F* (> 10) Resulted from the Analysis of Variance. Mineral Abbreviations are according to Table 1.

	F		*F*		*F*
Kln	191	Cs	46	Mn	20
Qtz	146	Ill	38	Si	19
CIA	86	Ca	32	> 63μm	15
Hem	82	Phy	31	Dol	12
Mg	76	Ti	30	Zr	12
P	74	Gt	30	Sb	12
K	62	Hf	21	Rt	12

breaking up of Pangea was accompanied by increased onshore humidity as seaways opened into the pangean interior with the installation of epicontinental seas [20] characterized by periods of sea incursion altering with long dry ones, where high evaporation rates dominated.

The presence of smectite, sepiolite and corrensite (See Table **1**) corroborate this interpretation [9]. Clay minerals associations, composed of marine Mg-rich minerals and detrital minerals, are in accordance with those formed in epicontinental regions of Western Europe [21, 22].

The presence of hematite indicates warm temperate to tropical areas, because it primarily occurs in well-drained areas and its formation is favored by warm dry conditions and small amounts of organic matter.

Phyllosilicates are more abundant in the Triassic-Hettangian clays due to the predominance of tiny granulometry with high proportion of the < 2 μm particle size, in average. Illite is the main clay mineral and has been interpreted as detrital, resulting from erosion of Carboniferous strata (slates and greywackes) without important chemical alteration of the inherited products [7]. Physical weathering as the main process to clays formation is also suggested by the low CIA values that characterize these samples, pointing to the prevailing of aridity conditions.

Mobile elements (K, Cs and P), probably associated with illite, are also very abundant and enable a good distinction between these clays and the Cretaceous ones. The enrichment in these elements indicates that these aged clays probably suffered post-depositional potassium metassomatism.

Cretaceous clays have high kaolinite, quartz and CIA contents. The granulometry is variable, but in general is coarser than in Triassic-Hettangian clays, with high proportion of sand fraction. This explains the high contents of Si, Zr and Hf (usually present as heavy minerals such as zircon) and Ti (in titanium oxides, such as rutile and anatase).

High quartz/phyllosilicate ratios, sometimes above the unit in several samples, confirm their siliciclastic character. In fact, these sediments resulted from fluvial discharges during Late Berriasian and Barremian, due to the tectonic instability associated to compressive movements.

The abundance of kaolinite is related with the high chemical weathering of felsic source rocks, as show the high CIA values. It is interpreted as to reflect episodes of enhanced humidity and high meteoric flow-through, which enabled leaching of most cations from the Paleozoic source area rocks, forming residual kaolinite.

Goethite is the typical iron oxide present in these units. Despite it can be formed under a broad range of climatic and hydrological conditions, a cool temperature and the presence of comparatively large amounts of organic matter, tend to favour goethite formation.

The typical association illite+kaolinite+goethite of these clays have been interpreted as a siderolithic facies related with erosion and transport of laterites under tropical climates; however, illite still prevails over kaolinite, suggesting hydrolysis was not extreme.

CONCLUSIONS

A detailed and independent geochemical and mineralogical study, mainly of the clay minerals associations, is indispensable to a valuable palaeoenvironmental interpretation of the depositional environment of the different clays. However, the illustrated example shows how multivariate analysis, namely PCA and K-means clustering, is helpful when exist varied and large amount of data and how the simultaneous analysis of geochemical, mineralogical and granulometric data enable the definition of the best discriminatory parameters, which can be used to emphasize some distinct palaeoenvironmental aspects between Triassic-Hettangian and Cretaceous clays.

The evaporitic transitional environment prevailing during deposition of Triassic-Hettangian clays is mainly evident by high contents of Mg, dolomite and hematite. Aridity conditions promoted physical weathering and formation of abundant illite. These Triassic clays were strongly transformed after deposition with incorporation of highly mobile elements (K, Cs and P).

The continental (fluvial) environment of deposition of Cretaceous clays is shown by high contents of kaolinite, which indicate proximity of clays with the source area and formation under conditions of humidity. High chemical al-

teration of felsic source rocks is also indicated by high CIA values.

ACKNOWLEDGEMENTS

As part of the Doctoral Program of M.J. Trindade, this work has been financially supported by the Fundação para a Ciência e Tecnologia (FCT) as a PhD fellowship (SFRH/BD/11020/2002). The authors would like to thank to the reviewers for their careful and constructive reviews that considerably improved the original manuscript.

REFERENCES

[1] Munhá, J. Metamorphic evolution of the South Portuguese Zone/Pulo do Lobo Zone, in *Pre-Mesozoic Geology of Iberia*; Dallmeyer, R.D.; Martínez García, E.; Eds.; Spring-Verlag: Berlin, **1990**, 363-368.

[2] Terrinha, P. Structural geology and tectonic evolution of the Algarve Basin, South Portugal, PhD thesis, Imperial College: London, **1998**.

[3] Terrinha, P.; Rocha, R.; Rey, J.; Cachão, M.; Moura, D.; Roque, C.; Martins, L.; Valadares, V.; Cabral, J.; Azevedo, M.R.; Barbero, L.; Clavijo, E.; Dias, R.P.; Gafeira, J.; Matias, H.; Matias, L.; Madeira, J.; Marques da Silva, C.; Munhá, J.; Rebelo, L.; Ribeiro, C.; Vicente, J.; Youbi, N. A Bacia do Algarve: *Estratigrafia, paleogeografia e tectónica, in Geologia de Portugal no Contexto da Ibéria*, Dias, R.P.; Araújo, A.; Terrinha, P.; Kullberg, J.C. Eds., University of Évora: Portugal, **2006**, 247-316.

[4] Martins, L.; Kerrich, R. Magmatismo toleítico continental no Algarve (sul de Portugal): um exemplo de contaminação crustal "in situ". *Comun. Inst. Geol. Mineiro*, **1998**, *85*, 99-116.

[5] Manuppella, G.; Moreira, J.B.; Grade, J.M.L.; Moura, A.A.C. Contribuição para o conhecimento das argilas do Algarve, Estudos: Notas e Trabalhos, **1985**, *27*, 59-76.

[6] Prates, S.C. O Cretácico detrítico do Algarve, PhD thesis, University of Lisbon: Portugal, **1986**.

[7] Hendriks, F.; Kellner, T.; Liebermann, L. Origin and evolution of Upper Triassic to Miocene clay-mineral associations from the eastern Algarve of Portugal. *Ciências da Terra*, **1988**, *9*, 129-140.

[8] Trindade, M.J.F.; Rocha, F.; Dias, M.I. Geochemistry and mineralogy of a Cretaceous sedimentary profile from central Algarve (Portugal). *J. Geochem. Explor*., **2006**, *88*, 450-453.

[9] Trindade, M.J.F. Geoquímica e mineralogia de argilas da Bacia Algarvia: transformações térmicas, PhD thesis, University of Aveiro: Portugal, **2007**.

[10] Heimhofer, U.; Adatte, T.; Hochuli, P.A.; Burla, S.; Weissert, H. Coastal sediments from the Algarve: low-latitude climate archive for the Aptian-Albian. *Int. J. Earth Sci*., **2008**, *97*, 785-797.

[11] Gouveia, M.A.; Prudêncio, M.I. New data on sixteen reference materials obtained by INAA. *J. Radioanal. Nucl. Chem.*, **2000**, *245*, 105-108.

[12] Schultz, L.G. Quantitative interpretation of mineralogical composition X-ray and chemical data for the Pierre Shale, *US Geol. Surv. Prof. Pap.*, **1964**, *391*, 1-31.

[13] Biscaye, P.E. Mineralogy and sedimentation of recent deep-sea clay in the Atlantic Ocean and adjacent seas and oceans. *Geol. Soc. Am. Bull*., **1965**, *76*, 803-832.

[14] Galhano, C.; Rocha, F.; Gomes, C. Geostatistical analysis of the influence of textural, mineralogical and geochemical parameters on the geotechnical behaviour of the "Argilas de Aveiro" formation (Portugal). *Clay Min*., **1999**, *34*, 109-116.

[15] Oliveira, A.; Rocha, F.; Rodrigues, A.; Jouanneau, J.; Dias, A.; Weber, O.; Gomes, C. Clay minerals from the sedimentary cover from the Northwest Iberian shelf. *Prog. Oceanogr.*, **2002**, *52*, 233-247.

[16] Shepard, F.P. Nomenclature based on sand-silt-clay ratios. *J. Sediment. Res.*, **1954**, *24*, 151-158.

[17] Nesbitt, H.W.; Young, G.M. Early Proterozoic climates and past plate motions inferred from major element chemistry of lutites. *Nature*, **1982**, *299*, 715-717.

[18] StatSoft, Inc., STATISTICA (data analysis software system), version 6. www.statsoft.com, **2003**.

[19] Dias. M.I.; Prudêncio, M.I. On the importance of using scandium to normalize geochemical data preceding multivariate analyses applied to archaeometric pottery studies. *Microchem. J.*, **2008**, *88*, 136-141.

[20] Manspeizer, W. The break-up of Pangea and its impact on climate: consequences of Variscan-Alleghanide orogenic collapse, in Palaeoclimate, Tectonics and Sedimentation during Accretion, Zenith, and Break-up of a Supercontinent; Klein G.D. Ed.; *Geological Society of America, Special Paper*, **1994**, *288*, 169-185.

[21] Rocha, F. Argilas aplicadas a estudos litoestratigráficos e paleoambientais na bacia sedimentar de Aveiro, PhD thesis, University of Aveiro: Portugal, **1993**.

[22] Weaver, C.E. *Clays, muds and shales, Developments in sedimentology*, v44. Elsevier: Amsterdam, **1989**.

Received: January 12, 2009 **Revised: May 06, 2009** **Accepted: May 06, 2009**